Analytical Methods

Accepted Manuscript

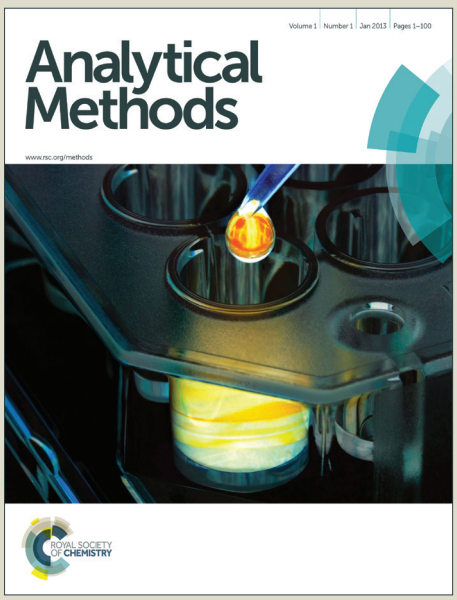

ROYAL SOCIETY OF CHEMISTRY

www.rsc.org/methods

Evaluation of Modified Fe_3O_4 Magnetic Nanoparticles Graphene for the Dispersive Solid-Phase Extraction to Determine the Trace PAHs in Seawater

Shaojun Zhang[1,2], Wanqing Wu[1*], Qinggong Zheng[1]

1 Marine Engineering College, Dalian Maritime University, 1 Linghai Road, 116026 Dalian, China

2 Maritime College, Shandong Jiaotong University, 115 Xinwei Road, 264200, Weihai, China

Abstract

In order to investigate the contamination caused by polycyclic aromatic hydrocarbons (PAHs) in seawater, Fe_3O_4 magnetic nanoparticles graphene (Fe_3O_4 MNG) was prepared and modified by micelle to act as an adsorbent for the solid-phase micro-extraction. The method showed satisfactory precision, reproducibility and linear response ($R^2 > 0.9981$) over the concentration range of 0.02 – 2.0 μg/L. Limits of detection of 16 PAHs ranged from 0.009 to 0.018 μg/L (*S/N*=3). The recovery of established method (79.01 - 99.67 %) was higher than that of the conventional solid-phase extraction method (29.27-88.04%). The enrichment factors of the PAHs were in the range of 53.85–103.64. The proposed method was successfully applied to determine PAHs in seawater samples collected from 56 different sites along the Bohai Sea in North China. The total concentrations of PAHs in seawater ranged between 54.90 - 8137.44 ng/L.

Keywords: magnetic nanoparticles graphene; micelle; solid-phase micro-extraction; polycyclic aromatic hydrocarbons; Bohai Sea

1. Introduction

Polycyclic aromatic hydrocarbons (PAHs) are a group of widely distributed and persistent organic pollutants (POPs) which include a number of carcinogenic compounds. Atmospheric deposition, river runoff and oil-spills are the three major types of PAHs sources adding to the marine pollution [1]. PAHs easily accumulate in seawater and efficiently spread

* Corresponding author. Tel.: +86 411 84724175; fax: +86 411 84724175.
E-mail address: wuwanqingdmu@sina.com (Wanqing Wu); dlmu212@163.com

throughout the marine food chain, thus possessing a high risk of affecting human health. "Mussel Watch" projects conducted in US and Asian coastal waters has provided information on the distribution of contamination caused by the PAHs on a global scale [2,3]. Based upon the analysis of samples collected from contaminated sites all over the world, high concentrations of PAHs have been reported in seawater (3500 ng/m^3) [4], sediments (30,200 ng/g dry weight) [5] and fish (512 ng/g) [6]. Bohai Sea is one of the most important economic finishing grounds in Northern China. However, ecological system of Bohai Sea has been on the verge of collapse due to a number of factors. Some of these factors include the eutrophication caused by the rivers, an intensive shipping line and a great number of offshore oilfields causing oil spills. Although, in recent years, a lot of research has focused on the contamination of Bohai Sea [7,8], yet the level of the pollution caused by PAHs is still largely unknown.

Due to the low sensitivity of the chromatographic technology, the possibility of obtaining direct measurements of the pollution caused by PAHs in contaminated marine waters is considered to be very difficult [9]. Therefore, pretreatment techniques including pre-concentration and column - cleaning processes are often required [10]. However, the analysis of the PAHs present in the seawater is still challenging due to a number of factors. Some of these factors include low concentrations, extremely complex chemistry and a number of unknown interferences. Results of many published reports differ widely from each other due to the fact that different analytical techniques were used in different, individual studies. Traditionally, liquid-liquid extraction (LLE) combined with solid-phase extraction (SPE) cleaning is the most common method for pretreatment of PAHs. Modern pretreatment techniques, such as the dispersive solid-phase extraction (DSPE), combine the extraction and cleaning processes into one step. Such techniques have greatly simplified the overall process and have quickly become an alternative method which can overcome the limitations of the classical techniques. In DSPE technique, based upon its selectivity and capacity, the adsorbent plays the most important role during extraction. Many researches have focused either on the synthesis or the modification of the specific nanomaterial adsorbents such as carbon nano-tubes (CNTs) [11], nanofibers [12] and graphene [13]. Graphene has large specific surface area (2360 m^2/g), high mechanical strength (1000 GPa) and fast electron transfer rate (200000 cm$^2\cdot$V$^{-1}\cdot$s^{-1}) [14]. A conjugated π-electron structure and hydrophobicity of graphene offers

additional affinity, thereby enhancing its interaction with the organic pollutants. Such enhancement in its interaction with the organic pollutants favors fast adsorption/desorption, making it a promising adsorbent material [15]. In the field of determination of PAHs, Wang et al. [16] used graphene oxide (GO) and reduced graphene for determination of naphthalene, one of the EPA's 16 priority pollutant PAHs. Shi et al. [17] used GO bound silica for SPE determination of 14 PAHs in cigarette smoke. However, during the process, the selectivity of the graphene is still not ideal, and large amounts of toxic organic solvents such as dichloromethane, acetonitrile, *n*-hexane and their mixtures are used. Use of such toxic solvents is harmful to human body while these can also act as secondary pollutants for the environment.

In this research, a surfactant coated Fe_3O_4 magnetic nanoparticles graphene (Fe_3O_4 MNG) composite was prepared and used as an adsorbent for DSPE process. Large specific surface area of graphene, which could form a platform for the micelle formations, can help improve the selectivity [18]. The extraction process could greatly be simplified by means of the collection of the adsorbent material using a magnet. The mechanism of this extraction process involves direct interaction between the micelles generated by the surfactant and the analytes on the graphene. The aggregates of surfactant molecules contain an inner core of water molecules and are dispersed in the medium. Thus, micelles are viewed as nanometer-scale microreactors. Micelle extraction have been used in a tremendous number of applications such as enhanced oil recovery, separation schemes such as liquid-liquid extraction processes, phase transfer catalysis, and various types of chemical reactions [19]. But using the nanomaterial as platform for the formation of micelle was seldom reported. Fe_3O_4 MNG was utilized as the stationary phase for the micelles and the solution was charged by adjusting the pH of the sample. Results from the proposed method were also compared with those of the classical SPE method. The proposed technique greatly simplifies the extraction process while still maintaining high sensitivity and high recovery rate. The Fe_3O_4 MNG@CTAB-DSPE-GC/MS method was utilized for detection of 16 EPA priority PAHs in 56 different contaminated samples collected from different sites along the Bohai Sea. The work is important for research community as it provides data which complement the current PAHs' pollution level in Bohai Sea and also provide technical support to the pollution control and

ecological remediation strategies.

2. Experimental

2.1. Chemicals and reagents

Methanol, acetonitrile, acetone and *n*-hexane were purchased from Merck Chemicals Pty. Ltd., Germany. Dodecyltrimethylammonium bromide (DTAB), cetyltrimethyl ammonium bromide (CTAB), sodium dodecyl benzene sulfonate (SDBS) and sodium dodecyl sulphate (SDS) were purchased from Aladdin Reagents (Shanghai) Co., Ltd., China. A standard mixture of the USA-EPA 16 priority PAHs (2000 μg/mL, dichloromethane) was purchased from Sigma-Aldrich Pty. Ltd., USA. The stock solution (10.0 mg/L) and working solutions were prepared using dichloromethane and were stored in a cool, dark refrigerator at 4 ˚C. Ammonia water (NH_3•H_2O), iron dichloride ($FeCl_2$•$4H_2O$) and hydrochloric acid (HCl) were purchased from the Damao Chemical Reagent (Tianjin) Co., Ltd., China. All solvents used in the gas chromatography–mass spectrometry (GC/MS, QP 2010 Plus, Shimadzu, Japan) were HPLC grade. Water used in the experiment was prepared by using a Milli-Q ultrapure water system (Millipore, USA).

2.2. Synthesis and characterization of Fe_3O_4 MNG

Fe_3O_4 MNG was prepared based upon the method proposed by Hummers with some modification [20]. The flow chart has been shown in Fig. 1. The Fe_3O_4 MNG was prepared by redox reaction using Fe_3O_4 MNPs and GO. Deionized water solution (40 mL) containing $FeCl_3 \cdot 6H_2O$ (60 mg), $FeCl_2$•$4H_2O$ (20 mg) and GO (80 mg) was purged by nitrogen using the Termovap Sample Concentrator (HP-5016SY, Shanghai, China) for 10 s to eliminate oxygen. The resultant solution was stirred and again purged with nitrogen. NH_3•H_2O was then added to the solution to maintain the pH at a value of 9 at 80 ℃. After 1 hour stirring, the color of the solution changed from yellow to black, indicating that the Fe_3O_4 MNG was successfully prepared. Fe_3O_4 MNG was collected by a magnet and was freeze-dried. The concentration of Fe_3O_4 MNG was 12.5 mg/mL. Scanning electron microscope (SEM, LEO1530, Zeiss, Germany), X-ray diffraction (XRD, 6000, Shimadzu, Japan), Fourier transform infrared

spectroscopy (FTIR, 8400S, Shimadzu, Japan) and vibrating sample magnetometer (VSM, Lake Shore 7410, USA) were used for characterization of the morphology, structure and magnetic properties of the Fe_3O_4 MNG.

2.3. Sample collection and extraction

Surface seawater samples were collected from 56 coastal sites along the Bohai Sea in May, 2015. All the samples were collected in brown sampling bottles and stored in 0 - 4 °C until extraction. The samples were filtrated through 0.45 μm micropore membranes. In this experiment, a nanomaterial supported micelle was prepared and used as an adsorbent for DSPE. Seawater sample solution (100 mL) was adjusted to a pH value of 3 by adding HCl to it. 1.0 mL of Fe_3O_4 MNG water solution (1.0 mg/mL) containing CTAB (1.0 mg/mL) was added to the sample solution. Extraction was continued for 20 min at room temperature. Fe_3O_4 MNG was collected by using a magnet. After liquid-desorption with 1.0 mL acetone, the acetone solution was analyzed by using GC/MS.

2.4. Chromatographic conditions

PAHs were separated by using a DB-5MS capillary column (30 m × 0.25 mm × 0.25 μm). Splitless injection mode was used with a volume of 1 μL. The column flow was set to 26.2 cm/sec. Electron impact (EI) mode was used in MS and the ion source temperature was 220 °C. GC/MS interface temperature was 250 °C. The column temperature was maintained at 70 °C for 1 min. The temperature was then raised to 300 °C by using a heating rate of 5 °C/min and maintained at 300 °C for 5 min. Later, the temperature was raised to 310 °C by using a heating rate of 5 °C/min and maintained at this value for 1 min. The mass spectrometry information of PAHs is shown in Table 1.

3. Results and discussion

3.1. Preparation and characterization of Fe_3O_4 MNG@CTAB

Fe_3O_4 MNG sheet was prepared under alkaline conditions with oxidation-reduction reaction using GO and Fe^{2+}. At room temperature, the reaction could be accomplished in one step. SEM characterization of GO is shown in Fig. 1a. Ultrathin GO was in the form of a

translucent slice. Its lateral dimensions ranged from tens of nanometers to a few microns. The SEM image of Fe_3O_4 MNG was shown in Fig. 1b. Fe_3O_4 magnetic nanoparticles (MNPs) were well-deposited on the surface of the GO surface and no occurrence of aggregates was observed. The average particle diameter of Fe_3O_4 MNPs was 10 nm. The SEM image (shown in Fig. 1c) of Fe_3O_4 MNG coated with CTAB (Fe_3O_4 MNG@CTAB) confirmed porous morphology of the adsorbent along with uniform size distribution of Fe_3O_4 MNG. This oxidation-reduction reaction did not need additional organic solvents. Therefore, no organic pollutants were introduced to the adsorbent. After the reaction, Fe_3O_4 MNG not only maintained the morphology of graphene, but also showed a good ability as a stationary phase carrier.

The magnetic properties of Fe_3O_4 MNG were determined by VSM. As shown in Fig. 2a, Fe_3O_4 MNG showed super paramagnetic character that made it a good adsorbent for the DSPE process. The maximum value for the saturation magnetization of Fe_3O_4 MNG was 51 emu/g, which was sufficient to analyze the PAHs present in the collected samples. Fe_3O_4 MNG sheets were rapidly dispersed after exposure to the external magnetic field. This phenomenon was caused due to the reason that the Fe_3O_4 MNG had large number of polar functional groups which not only provided abundant adsorption sites for micelles but also improved the dispersion of Fe_3O_4 MNG in water. The magnetic properties of Fe_3O_4 MNG@CTAB were also determined. The maximum saturation magnetization was slightly decreased to 44 emu/g, which was still sufficient to analyze the PAHs in the samples. The dispersion system of Fe_3O_4 MNG in water remained stable at room temperature for 30 days. The magnetic characteristics of Fe_3O_4 MNG also remained intact and showed no signs of variation.

Zeta potential of pH 3 - 11 in Fe_3O_4 MNG has been shown in Fig. 2b. Zeta potential of Fe_3O_4 MNG was 6.8 mV at a pH value of 3. When pH was increased to a value of 7, Zeta potential reduced to -15.0 mV. As pH increased to 11, Zeta potential did not show significant changes, which indicated the saturation of the negative charges. Zeta potentials of GO, Fe_3O_4 MNPs, Fe_3O_4 MNG and Fe_3O_4 MNG were also compared. Zeta potential of Fe_3O_4 MNG@CTAB was similar to Fe_3O_4 MNG, which indicated the supporting of micelle did not affect its performance. Fe_3O_4 MNPs was positively charged under acidic conditions (pH < 7)

while it became negatively charged under alkaline conditions (pH > 7). GO was negatively charged for pH values ranging from 3 to 11. Just like GO, Fe_3O_4 MNG was negatively charged for almost all pH conditions studied. Therefore, in determination of magnetic properties of Fe_3O_4 MNG, GO played a more significant role than Fe_3O_4 MNPs.

FTIR spectroscopy has been used to explore the molecular adsorption, transmission and the creation of a molecular character of the prepared material. As shown in Fig. 2c, the vibrational band assignments (cm^{-1}) of the GO were summarized as follows: 1725 (C=O), 1620 (C=C), 1375 (C-O), 1224 (C-O), 1040 (C-O). The peak comparison between GO and Fe_3O_4 MNG showed that oxygen functional groups were almost entirely removed. XRD spectroscopy of Fe_3O_4 MNG and Fe_3O_4 MNG@CTAB showed that the characteristic peaks of GO had disappeared and at 18.2° (111), a diffraction peak representing the graphene crystal width had appeared. The peak indicated that in the reaction process, most of the oxygen functional groups have been reduced. The obtained graphene sheet layer showed irregular stacking and decreased crystal structural integrity. Characteristic peaks of magnetite were observed at 2θ of 18.2° (111), 30.1° (220), 35.4° (311), 43.02° (400), 53.4° (422), 57° (511), 62.6° (440) and 73.9° (553). Sherrer formula was used to calculate the average particle size of Fe_3O_4 particles in the catalyst samples. According to the half-height of Fe_3O_4 (220), (311) (400), (511), (440), the average particle size was determined to be 40 nm.

3.2. Optimization of the extraction procedure

3.2.1. Investigation of the surfactant

In order to obtain higher adsorption capacity for PAHs, cationic (DTAB and CTAB) and anionic (SDS and SDBS) surfactants were added to act as modifiers to form micelles. PAHs recoveries of cationic surfactants were higher than the anionic surfactants. CTAB obtained the highest recovery, which indicated that CTAB was the most suitable surfactant for the extraction of PAHs. The phenomenon can be explained by reasoning that the hydrocarbon chains of CTAB interact with PAHs whose weakly polar groups cause the interactions through the electrostatic or hydrogen bonds. Hence the micelle extraction technology was suitable for application to the DSPE process. The surfactant molecule consists of a

hydrophilic (water-loving) head and a hydrophobic (water-hating) tail. The formation of CTAB micelles in Fe_3O_4 MNG was studied through the determination of critical micelle concentration (CMC) (Fig. 3a). The concentration of the surface active agent increased to the CMC and that was when, the interaction between the opposite surface charges presented in the surfactant and the nanomaterial took place [21]. Hence, formation and deposition of the initial micelle took place on the surface of the nanomaterial. The tail of the hydrophobic part of the micelle was exposed to aqueous solution. The Fe_3O_4 MNG surface modified by the surfactant was changed into a hydrophobic entity and thus became favorable to adsorb weakly polar organic compounds. In view of the large surface area of Fe_3O_4 MNG and the number of active hydroxyl groups present, the adsorption capacity of PAHs after the modification by CTAB was greatly improved.

3.2.2. Effect of CTAB concentration and sample volume

The optimization of CTAB concentration in Fe_3O_4 MNG was studied by the determination of the recovery rate. The concentration of CTAB ranged from 0.0 to 1.5 mg/mL. As shown in Fig. 3b, in the absence of CTAB (concentration of 0.0 mg/L), the extraction efficiency was poor and only a little part of PAHs could directly be extracted. Even for a pH value of 3, when the Fe_3O_4 MNG was positively charged, the electrostatic attractions between Fe_3O_4 MNG and PAHs were still weak, resulting in low extraction efficiency. Therefore, it can be said that in the absence of a surfactant, Fe_3O_4 MNG was not an ideal ionic compound adsorbent. Later, the concentration of CTAB was increased from 0.0 to 0.6 mg/L. For a concentration of 0.6 mg/L, the recoveries increased remarkably, indicating that the micelles had formed on the surface of Fe_3O_4 MNG plate. The maximum extraction efficiency reached a value of 1.0 mg/mg (CTAB/MNG). At this concentration, CTAB micelles were adsorbed on the Fe_3O_4 MNG, thus providing the highest adsorption of PAHs. It also indicated that the surface of the Fe_3O_4 MNG was saturated with CTAB. However, a further increase in the concentration of CTAB did not result in a significant change in the adsorption capacity. The reason for a small change was that, with the formation of the PAHs, free micelles were also formed in the solution. Some of the PAHs were adsorbed on these free micelles. Therefore, it indicated the highest adsorption capacity of Fe_3O_4 MNG@CTAB and had a value of about 1.0 mg/mg

(CTAB/MNG).

The sample volume also affected the extraction efficiency. When sample volume was increased from 50 mL to 100 mL, a small change in adsorption capacity was observed. However, when the sample volume was increased to 150 mL, significant drop in recovery was observed. Therefore, it was concluded that 1.0 mg/mg (CTAB/MNG) was capable to adsorb PAHs in a 100 mL volume of the sample.

3.2.3. Influence of the ionic strength, sample pH and equilibrium time

In the sample solution, the ionic strength of the medium increases with the adding of the ionic strength, while the solubility of PAHs is decreased so that the extraction quantity is increased thus the extraction efficiency improved. Sodium chloride and sodium sulfate (0-15%, v/v) was added as the ionic strength modifier in the present work. But the ionic strength has little effect on the extraction efficiency, so the influence of ionic strength was ignored in this research.

In the sample solution, pH determines the form of the analyte. Therefore pH value of the sample will affect the extraction efficiency. Sample pH in the range of 4 to 11 was investigated. The adsorption of PAHs reached a maximum for a pH value was 6.8. The reason was that CTAB was an amphoteric oxide with isoelectric point of 6.2. When pH value was higher than the isoelectric point, Fe_3O_4 MNG surface was covered with negative charge, thereby due to the electrostatic attraction, reacted with the cations. Since the negative charge was beneficial to the adsorption of the cationic surfactant, the maximum adsorption occurred at a pH value which was higher than the isoelectric point of the Fe_3O_4 MNG. Therefore, when the sample pH had a value of about 6.8, all the PAHs were easily adsorbed. Generally, the environmental water samples had a neutral pH, so a pH value of 6.8 was selected for the DSPE process.

Equilibrium time is another important factor to determine the extraction efficiency. The extraction time was investigated by doing experiments in a time range of 5 - 30 min. The recovery of PAHs increased in the first 20 min. With further increase in equilibrium time, no remarkable change was observed. This indicated that the micelle formation process was fast. In fact, 20 min time was sufficient to achieve both equilibrium and satisfactory extraction

efficiency. Therefore, to ensure the complete adsorption, an equilibrium time of 20 min was chosen.

3.2.4. Effect of desorption solvent type and the time

The purpose of the elution was to desorb CTAB micelles from the Fe_3O_4 MNG plate, thereby releasing the analyte into the elution solution. The effect of elution solvent on Fe_3O_4 MNG@CTAB was studied by measuring the recovery rate. Four organic solvents, acetonitrile, methanol, acetone and dichlorine were tested. Acetone shows a more profound and favorable effect than all the other solvents. Thus, acetone was used as the elution solvent in the desorption experiments. In the DSPE process, ideally both the the adsorption and desorption processes should have fast kinetics. In order to achieve complete desorption of PAHs from Fe_3O_4 MNG, desorption time (in a range of 0-15 min) was examined. The best desorption results were achieved for a time of 6 min. Therefore, 6 min was chosen as the desorption experiments.

3.2.5 Comparison of Fe_3O_4 MNG@CTAB with Fe_3O_4 MNPs@CTAB

Performances of the Fe_3O_4 MNG and Fe_3O_4 MNPs as the solid phase carrier of micelles were also evaluated. The formation of Fe_3O_4 MNG micelles was found at pH 6.8 that achieved the highest adsorption (1.0 mg/mg). In comparison, the formation of Fe_3O_4 MNPs micelles was found at pH 9.6 that achieved the highest adsorption (0.9 mg/mg). As environmental water samples usually in neutral conditions, the Fe_3O_4 MNG@CTAB could facilitate extraction. At the same conditions, the obtained recovery rate of Fe_3O_4MNG@CTAB at a pH value of 6.8 (79.01-99.67%) was much higher than that of Fe_3O_4 MNPs@CTAB at a pH value of 9.6 (15.27-56.45%). Additionally, the dispersion of Fe_3O_4 MNG@CTAB in aqueous solution was more stable than Fe_3O_4 MNPs@CTAB. After 30 days of observation, no significant change in magnetism was observed. On the other hand, for the Fe_3O_4 MNPs@CTAB solution, showed a sharp decline in magnetism. The results showed that Fe_3O_4MNG@CTAB provided more significant advantages than Fe_3O_4 MNPs@CTAB and therefore, it was more favorable for the pretreatment of seawater samples.

3.3. Method validation

Table 2 summarizes the results which validate the proposed method. These results include the determined values of linear range, correlation coefficient (R^2), relative standard deviation (RSD), minimum limit of detection (LOD), limit of quantitation (LOQ) and spiked recovery.

3.3.1. Linear range, LOD and recovery

Satisfactory correlation coefficient ($R^2 > 0.9981$) was observed between the peak area and the concentration of PAHs in the range of 0.02 – 2.0 μg/L. Values for the LOD and LOQ of Fe_3O_4 MNG@CTAB DSPE method were in the ranges of 0.009 - 0.018 μg/L (S/N=3) and 0.01 - 0.002 μg/L respectively. These results showed that the proposed method achieved a high precision. The results were satisfactory with the spiked recoveries in the range of 79.01 - 99.67 %. The analysis time was 50 minutes. As the sample solution included a small portion of other organic pollutants, the real samples had some impurity peaks as compared to the standard PAHs spectrum. In consideration of CTAB may be has some negative interference to the GC capillary column and detector, a comparison of with/without CTAB experiment was carried out in the SIM mode. The detection result showed that the interference of CTAB was negligible. All the samples were detected using CTAB as modifier, no obvious contamination was found towards the capillary column and detector. Quantitative analysis of PAHs took less than 30 min for the sample pretreatment and the LOD value approached the trace level.

3.3.2. Variability of analysis method

Instrument stability was assessed by continuously analyzing the calibration verification standards every 6 samples. Considering the variability of analysis method, a real sample S52 (with two parallel sample tests) was tested daily for three days (n=9). Values for average and standard deviation were then calculated. As is shown in the final column of the Table 2, the variations were insignificant. The inter-day precision for three different days showed a variation of less than ± 10%. The enrichment factors of the PAHs were in the range of 53.85–103.64. The results showed that after the Fe_3O_4 MNG@CTAB DSPE method, GC/MS in SIM mode was a reliable method for monitoring the PAHs at very low concentrations.

3.3.3. Comparison of DSPE with LLE-SPE procedure

The traditional LLE-SPE procedure consisted of the following steps. Initially, a 250 mL sample was extracted by using 20 mL mixture of dichloromethane:actone (1:1) for 30 min. The extraction process was repeated twice. After centrifugation at 4000 rpm and 0 °C for 5 min, the supernatant was cleaned by SPE cartridges (Agilent Zorbax C_{18}, 0.2 g, 3 mL polypropylene) using a 20 mL mixture of dichloromethane: acetone (1:1). The cleaned solution was purged and dried by nitrogen in a Termovap Sample Concentrator. The residue was dissolved in 1.0 mL acetone for GC/MS analysis. The recoveries of PAHs ranged from 29.27 % to 88.04 %, which were significantly lower than those resulted from Fe_3O_4 MNG@CTAB DSPE method (and had values in the range of 79.01 - 99.67 %). Therefore, the spiked recoveries of PAHs analysis increased by around 1.13 - 2.71 times. A real sample S52 was analyzed for comparison. The TPAH was 1751.62 ng/L. Comparing the data of 2430.15 ng/L obtained by the proposed method, the results showed that in the traditional process 27.92 % of PAHs were lost. This showed that Fe_3O_4 MNG@CTAB has higher adsorption efficiency.

3.4. Application of the method to the analysis of Bohai Sea samples

Seawater samples from 56 different locations along the Bohai Sea, North China were collected. Bohai Sea collects large amounts of PAHs from atmospheric deposition, river runoff, industrial discharge and oil-spills coming from the offshore oilfields. The total concentration of PAHs (TPAH) of *Laizhou Bay (S01-S11), Bohai Bay (S12-S21) and Liaodong Bay (S22-S56)* ranged from 54.90 to 8137.44 ng/L (details see Table 3). TPAH concentrations at S16 (4264.03 ng/L), S50 (4571.73) and S51 (5382.18 ng/L) are much higher than those at other stations. Among these, S16 is important as it is located in the *Bohai Bay*, west of the Bohai Sea. The pollution of *Bohai Bay* is mostly caused by the Yellow River which has a high concentration of pollutants. It also has a large number of offshore oilfields. Station S50 and S51 are located in a shallow, half closed bay called Dalian's *Jinzhou Bay*. On *Jinzhou Bay*, an artificial island of 21 km^2 is being developed which would later host an offshore airport. Four samples were selected from *Jinzhou Bay*. The concentrations of TPAHs were observed to be 607.04 ng/L (S49), 4571.73 ng/L (S50), 5382.18 ng/L (S51) and 2430.15

ng/L (S52) respectively. The results show that this area is heavily polluted due to large industrial activities. The average concentrations of PAHs in seawater of *Bohai Bay* (1445.56 ng/L, ranging from 251.26 to 4264.03 ng/L) are 1.76 times higher than the *Liaodong Bay* (819.56 ng/L, ranging from 54.97 to 5382.18 ng/L) and 2.3 times higher than the *Laizhou Bay* (627.60 ng/L, ranging from 33.02 to 1610.71 ng/L). Obviously, the concentration levels of PAHs in Bohai Sea are much higher than the values reported 10 years ago [22]. The 16 PAHs are grouped into low-molecular weight PAHs (LMW) (having 2 – 3 rings) and high-molecular weight (HMW) PAHs (having 4 – 6 rings). High concentrations of LMW were observed. This was especially true for 3-ringed LMW PAHs such as PHE, ANT and FLT which were the dominating PAHs in seawater. The sum of PHE, ANT and FLT accounted for 8.79 %, 10.86 % and 39.88 % of TPAHs.

Conclusions

In this work, Fe_3O_4 MNG was synthesized along with the micelle extraction and was used as a novel adsorbent to develop DSPE analysis. Fe_3O_4 MNG@CTAB exhibited good adsorption ability for PAHs. The recovery of proposed method (79.01 - 99.67 %) was higher than that of the conventional SPE method (29.27 - 88.04 %). Therefore, the spiked recovery increased by about 1.13 - 2.71 times. The method was successfully applied to the analysis of the seawater. The average concentrations of PAHs in seawater of *Bohai Bay* (1445.56 ng/L) are 1.76 times higher than those for the *Liaodong Bay* (819.56 ng/L) and 2.3 times higher than the values for the *Laizhou Bay* (627.60 ng/L). PHE, ANT and FLT, all of which contain three rings and constitute the LMW PAHs, were dominant PAHs in the seawater and accounted for 8.79 %, 10.86 % and 39.88 % of TPAHs respectively. The work not only presents up-to-date information on the high concentrations of several carcinogenic PAHs in Bohai Sea, but also proposes a novel graphene-based analysis method which serves as a useful contribution to the already existing literature.

References

[1] ATSDR, Toxicological profile for polycyclic aromatic hydrocarbons (PAHs) (update).

Atlanta, GA: Agency for Toxic Substances and Disease Registry, 1995.

[2] T.L. Wade, J.L. Sericano, P.R. Gardinali et al., 'Mussel Watch' project: Current use organic compounds in bivalves. *Mar. Pollut. Bull.,* 1998, 37(1), 20-26.

[3] G.G. Lauenstein, Comparison of organic contaminants found in mussels and oysters from a current mussel watch project with those from archived mollusc samples of the 1970s. *Mar. Pollut. Bull.*, 1995, 30(12), 826-833.

[4] C.C. Hung, F.C. Ko, G.C. Gong, et al., Increased zooplankton PAH concentrations across hydrographic fronts in the East China Sea. *Mar. Pollut. Bull.*, 2014, 83(1), 248-257.

[5] H. Nakataa, K. Ueharaa, Y. Gotoa et al., Polycyclic aromatic hydrocarbons in oysters and sediments from the Yatsushiro Sea, Japan: Comparison of potential risks among PAHs, dioxins and dioxin-like compounds in benthic organisms. *Ecotoxicol. Environ. Saf.*, 2014, 99, 61-68.

[6] Z.H. Zhao, L. Zhang, Y.J. Cai et al., Distribution of polycyclic aromatic hydrocarbon (PAH) residues in several tissues of edible fishes from the largest freshwater lake in China, Poyang Lake, and associated human health risk assessment. *Ecotoxicol. Environ. Saf.*, 2014, 104, 323-331.

[7] L.M. Hu, Z.G. Guo, J.L. Feng et al., Distributions and sources of bulk organic matter and aliphatic hydrocarbons in surface sediments of the Bohai Sea, China. *Mar. Chem.*, 2009, 113, 197-211.

[8] M. Ma, Z. Feng, C. Guan et al., DDT, PAH and PCB in sediments from the intertidal zone of the Bohai Sea and the Yellow Sea. *Mar. Pollut. Bull.*, 2001, 42, 132–136

[9] N.X. Ma, W. Bian, R.J. Li, et al. Quantitative analysis of nitro-polycyclic aromatic hydrocarbons in PM2.5 samples with graphene as a matrix by MALDI-TOF MS. *Anal. Methods*, 2015, **7**, 3967-3971.

[10] S.N. Egli, E.D. Butler, C.B. Bottaro, Selective extraction of light polycyclic aromatic hydrocarbons in environmental water samples with pseudo-template thin-film molecularly imprinted polymers. *Anal. Methods*, 2015, 7, 2028-2035.

[11] E. Bet-moushoul, Y. Mansourpanah, Kh. Farhadi et al., TiO2 nanocomposite based polymeric membranes: A review on performance improvement for various applications in chemical engineering processes. *Biochem. Eng. J.*, 2016, 283, 29-46.

[12] J. Huang, H.T. Deng, D.D. Song et al., Electrospun polystyrene/graphene nanofiber film as a novel adsorbent of thin film microextraction for extraction of aldehydes in human exhaled breath condensates. *Anal. Chim. Acta*, 2015, 878, 102-108.

[13] M.N.M. Zubir, A. Badarudin, S.N. Kazi et al., Experimental investigation on the use of reduced graphene oxide and its hybrid complexes in improving closed conduit turbulent forced convective heat transfer. *Exp. Therm. Fluid. Sci.*, 2015, 66, 290-303.

[14] S.J. Abraham, N. R. Nirala, S. Pandey, et al., Functional graphene–gold nanoparticle hybrid system for enhanced electrochemical biosensing of free cholesterol. *Anal. Methods,* 2015, **7**, 3993-4002.

[15] Z.H. Shi, J.D. Hu, Q. Li, et al., Graphene based solid phase extraction combined with ultra high performance liquid chromatography–tandem mass spectrometry for carbamate pesticides analysis in environmental water samples. *J. Chromatogr. A.*, 2014, 1355, 219-227.

[16] J. Wang, B.L. Chen. Adsorption and coadsorption of organic pollutants and a heavy metal by graphene oxide and reduced graphenematerials. *Chem. Eng. J.*, 2015, 281, 379-388.

[17] R. Shi, L.H. Yan, T.G. Xu et al., Graphene oxide bound silica for solid-phase extraction of 14 polycyclic aromatic hydrocarbons in mainstream cigarette smoke. *J. Chromatogr. A.*, 2015, 1375, 1-7.

[18] H. Sun, J.P. Lai, Y.S. Fung, Simultaneous determination of gaseous and particulate carbonyls in air by coupling micellar electrokinetic capillary chromatography with molecular imprinting solid-phase extraction. *J. Chromatogr. A.*, 2014, 1358, 303-308.

[19] M. Hryniewicka, B. Starczewska, The usage of micellar extraction for analysis of fluvastatin in water and wastewater samples. *J. Pharm. Biomed. Anal.*, 2015, 106, 129-135.

[20] Q. Liu, J.B. Shi, T. Wang, Hemimicelles/admicelles supported on magnetic graphene sheets for enhanced magnetic solid-phase extraction. *J. Chromatogr. A.*, 2012, 1257, 1-8.

[21] Y.F. Zhang, H.K. Lee, Low density solvent based vortex assisted surfactant enhanced emulsification liquid–liquid microextraction combined with gas chromatography–mass spectrometry for the fast determination of phthalate esters in bottled water. *J. Chromatogr. A.*, 2013, 1274, 28-35.

[22] J.Y. Hu, Y. Wan, B. Shao et al. Occurrence of trace organic contaminants in Bohai Bay and its adjacent Nanpainu River, North China. *Mar. Chem.,* 2005, 95, 1–13.

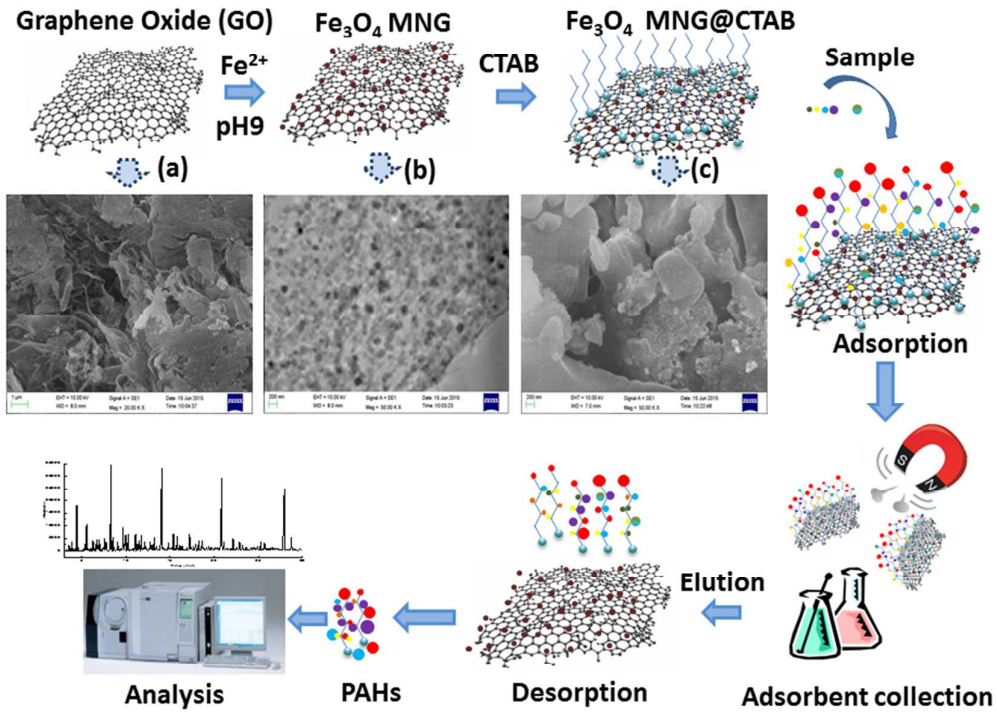

Fig. 1. Scheme diagram of Fe_3O_4 MNG synthesis and SPME procedures.

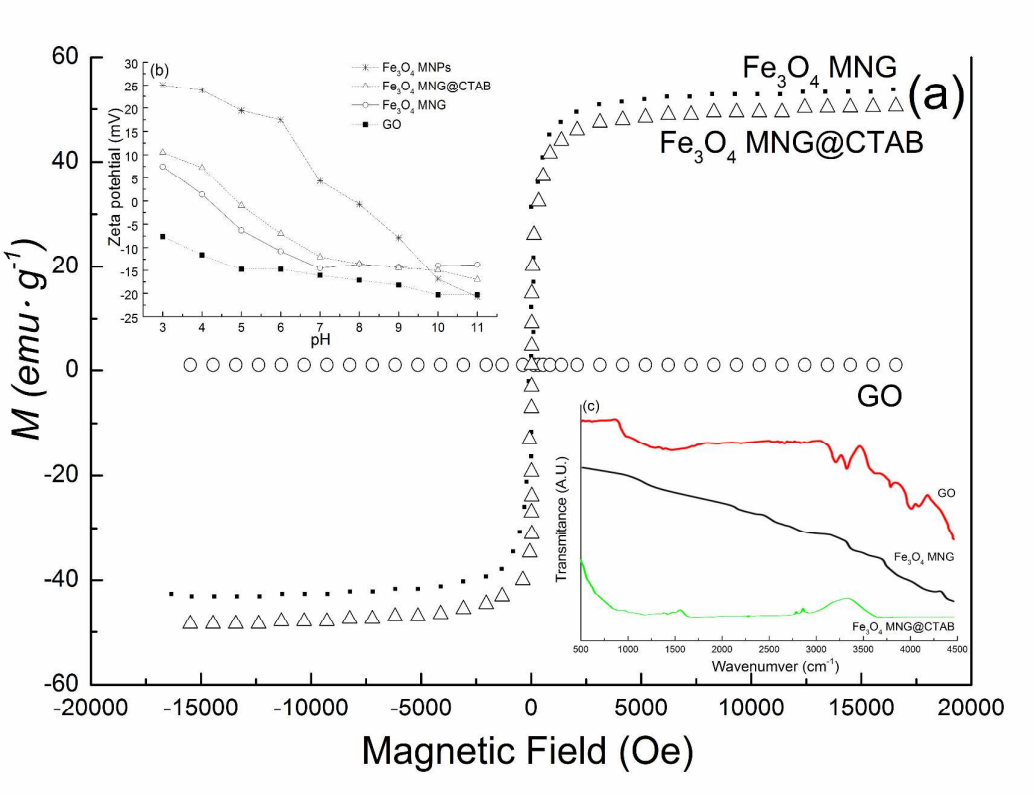

Fig. 2 Characterization of the proposed adsorption material: (a) magnetic hysteresis loop; (b) Zeta potentials of Fe_3O_4 MNPs, Fe_3O_4 MNG@CTAB, Fe_3O_4 MNG and GO; (c) FTIR spectroscopy of GO, Fe_3O_4 MNG and Fe_3O_4 MNG@CTAB.

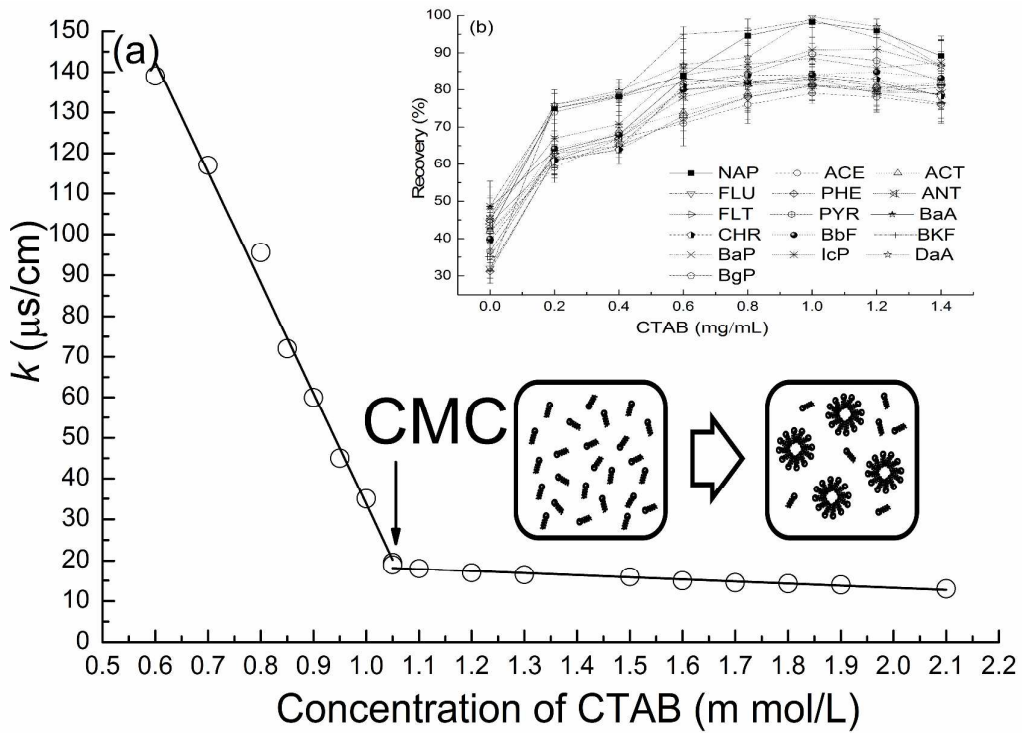

Fig.3 (a) Critical micelle concentration (CMC) of CTAB; (b) Effect of CTAB concentration on adsorption.

Table 1 Parameters of PAHs in GC/MS analysis

PAHs	Abb.	MF	MW	RT	Qualitative ion	Reference ion
Naphthalene	NAP	$C_{10}H_8$	128	4.681	128	102,64
Acenaphthylene	ACE	$C_{12}H_8$	152	7.292	152	126,76
Acenaphthene	ACT	$C_{12}H_{10}$	154	7.711	154	126,76
Fluorene	FLU	$C_{13}H_{10}$	166	9.053	166	139,82
Phenanthrene	PHE	$C_{14}H_{10}$	178	12.440	178	152,89
Anthracene	ANT	$C_{14}H_{10}$	178	12.706	178	152,89
Fluoranthene	FLT	$C_{16}H_{10}$	202	18.731	202	106,92
Pyrene	PYR	$C_{16}H_{10}$	202	17.702	202	174,101
Benz(a)anthracene	BaA	$C_{18}H_{12}$	228	24.680	228	114,101
Chrysene	CHR	$C_{18}H_{12}$	228	24.870	228	114,101
Benzo(b)fluoranthene	BbF	$C_{20}H_{12}$	252	31.010	252	126,113
Benzo(k)fluoranthene	BkF	$C_{21}H_{14}$	266	29.828	252	253,125
Benzo(a)pyrene	BaP	$C_{20}H_{12}$	252	29.637	252	126,113
Indeno(1,2,3-cd)pyrene	IcP	$C_{22}H_{12}$	276	35.050	276	138,124
Dibenz(a,h)anthracene	DaA	$C_{22}H_{14}$	278	35.242	278	139,124
Benzo(g,h,i)perylene	BgP	$C_{22}H_{12}$	276	36.005	276	138,124

Abb: Abbreviation, MF: molecular formula, MW: Molecular Weight, RT: retention time

Table 2 Method validation of Fe_3O_4 MNG@CTAB as adsorbent for DSPE followed by GC/MS analysis

Abb.	LR (μg/L)	R^2	LOD (μg/L)	Recovery (%)	RSD (%)	Variability (μg/L)
NAP	0.02-2.0	0.9981	0.018	79.01	1.34	470.12±34.5
ACE	0.02-2.0	0.9985	0.016	81.32	0.13	116.32±10.23
ACT	0.02-2.0	0.9986	0.018	80.98	1.18	155.12±13.54
FLU	0.02-2.0	0.9990	0.015	81.24	0.75	332.47±21.25
PHE	0.02-2.0	0.9994	0.013	81.22	1.24	317.51±12.36
ANT	0.02-2.0	0.9992	0.016	82.95	0.81	118.51±9.45
FLT	0.02-2.0	0.9998	0.010	83.13	0.53	828.45±7.21
PYR	0.02-2.0	0.9997	0.012	83.57	0.43	50.12±3.01
BaA	0.02-2.0	0.9994	0.014	84.16	0.64	41.53±2.51
CHR	0.02-2.0	0.9991	0.010	84.26	0.56	<LOD
BbF	0.02-2.0	0.9995	0.009	98.87	0.27	<LOD
BkF	0.02-2.0	0.9994	0.010	88.55	0.68	<LOD
BaP	0.02-2.0	0.9991	0.009	90.81	0.94	<LOD
IcP	0.02-2.0	0.9998	0.010	99.67	0.36	<LOD
DaA	0.02-2.0	0.9994	0.010	89.78	0.80	<LOD
BgP	0.02-2.0	0.9993	0.010	98.19	0.52	<LOD

Abb: Abbreviation, LR: Linear range, SR: Spiked recovery

Table 3 PAHs distributed in seawater along Bohai Sea, China

PAHs	Ring	TPAH (ng/L)	Average TPAH (ng/L)	TPAH (ng/L)	Average TPAH (ng/L)	TPAH (ng/L)	Average TPAH (ng/L)
		Laizhou Bay		*Bohai Bay*		*Liaodong Bay*	
NAP	2	351.67	31.97	158.42	15.84	1721.04	49.17
ACE	3	853.66	77.61	979.63	97.96	2686.32	76.75
ACT	3	778.91	70.81	849.36	84.94	2602.73	74.36
FLU	3	602.21	54.75	1154.72	115.47	2570.30	73.44
PHE	3	624.02	56.73	1100.95	110.09	2848.87	81.39
ANT	3	661.34	60.12	1285.45	128.54	3688.16	105.38
FLT	3	1189.91	108.17	10230.99	1023.10	10352.66	295.79
PYR	4	293.99	26.73	41.033	4.10	481.75	13.76
BaA	4	65.8	5.98	72.35	7.23	66.55	1.90
CHR	4	11.52	1.05	75.43	7.54	756.23	21.61
BbF	5	510.47	46.41	-	-	125.52	3.59
BkF	5	1102.7	100.25	204.95	20.49	91.81	2.62
BaP	5	-	-	-	-	-	-
IcP	6	95.65	8.69	-	-	692.57	19.79
DaA	6	-	-	-	-	-	-
BgP	6	-	-	-	-	-	-

Laizhou Bay (S01-S11); *Bohai Bay* (S12-S21); *Liaodong Bay* (S22-S56). -: <LOD

Table of contents entry

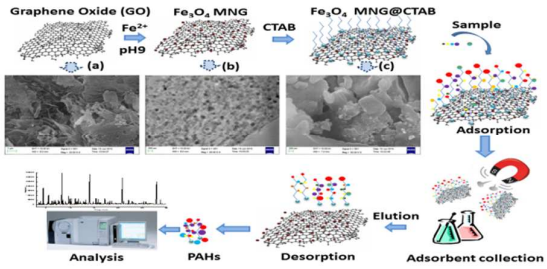

A novel Fe_3O_4 MNG@CTAB composite was prepared as DSPE adsorbent for determination of PAHs contaminant in seawater.